Submitted to *INFORMS Journal on Computing*
manuscript (Please, provide the manuscript number!)

Authors are encouraged to submit new papers to INFORMS journals by means of a style file template, which includes the journal title. However, use of a template does not certify that the paper has been accepted for publication in the named journal. INFORMS journal templates are for the exclusive purpose of submitting to an INFORMS journal and should not be used to distribute the papers in print or online or to submit the papers to another publication.

arXiv:1703.05206v2 [cs.SY] 19 Mar 2017

A Modified Benders Decomposition for Chance-Constrained Unit Commitment with N-1 Security and Wind Uncertainty

Kaarthik Sundar[†], Harsha Nagarajan[†], Line Roald[†], Sidhant Misra[†], Russell Bent[†], Daniel Bienstock[‡]
† Center for Non-Linear Studies, Los Alamos National Laboratory, Los Alamos, NM. Contact: rbent@lanl.gov
‡ Department of Industrial Engineering and Operations Research and Department of Applied Physics and Applied Mathematics, Columbia University, NY.

As renewable wind energy penetration rates continue to increase, one of the major challenges facing grid operators is the question of how to control transmission grids in a reliable and a cost-efficient manner. The stochastic nature of wind forces an alteration of traditional methods for solving day-ahead and look-ahead unit commitment and dispatch. In particular, the variability of wind generation increases the risk of unexpected overloads and cascading events. To address these questions, we present an N-1 Security and Chance-Constrained Unit Commitment (SCCUC) that includes models of generation reserves that respond to wind fluctuations and models of tertiary reserves that respond to single component outages. We formulate the SCCUC as a mixed-integer, second-order cone problem that limits the probability of failure. We develop a modified Benders decomposition algorithm to solve the problem to optimality and present detailed case studies on the IEEE RTS-96 three-area and the IEEE 300 NESTA test systems. The case studies assess the economic impacts of contingencies and various degrees of wind power penetration and demonstrate the effectiveness and scalability of the algorithm.

Key words: N-1 security; unit commitment; chance-constraints; Benders decomposition; wind energy

1. Introduction

Transmission grids play a vital role in the reliable and economically efficient operation of electric power systems. As renewable energy penetration rates continue to grow, the stochastic nature of renewable generation necessitates an alteration of traditional methods for solving day-ahead and look-ahead Unit Commitment (UC) and generation dispatch. The fluctuations caused by wind and solar generation can bring system components closer to their physical limits or cause unforeseen overloads in real-time operation. This reduces the ability to adequately handle contingencies and increases operational risk. As a result, power system operators are interested in securing the grid against component failures in the presence of these fluctuations.

More formally, the security of a power grid is defined by its ability to survive contingencies (Kundur et al. (2004)). The failure to secure a power system could potentially result in cascading events and large scale blackouts (Andersson et al. (2005), CIGRE (2009)). The N-1 security criterion was developed to avoid such incidents (see Stott et al. (1987) and references therein). While N-1 is an important security criteria, it is only well defined for a deterministic operating condition. With uncertainty from wind and solar power, the system might face considerable risk from cascading events in real-time operation, even though the system was N-1 secure for the forecast operating condition. Thus, there is a need for methods that appropriately limit the risk from uncertain deviations.

The literature considers a number of approaches to handle uncertainty in power systems operational planning, including two-stage and multi-stage stochastic programming approaches (Bouffard and Galiana (2008), Morales et al. (2009), Uçkun et al. (2016)), robust models (Lorca and Sun (2015), Warrington et al. (2013)) and chance-constrained formulations (Margellos et al. (2013), Vrakopoulou et al. (2013a), Roald et al. (2013), Bienstock et al. (2014)). Here, we use the latter approach, as chance constraints allows for a comprehensive, yet computationally tractable uncertainty representation and aligns well with several methods applied in industry. Industry practices that are naturally represented through chance constraints include probabilistic reserve dimensioning (applied in ENTSO-E ENT (2013)) and the definitions of reliability margins for flow-based market coupling in parts of Europe (see CWE (2011)). We develop a comprehensive model that incorporates all aspects of day-ahead planning and security discussed above - UC for generators, N-1 security constraints for line and generator outages, chance constraints to ensure stochastic security with respect to wind, generation reserves, and tertiary (spinning) reserves. We refer to this problem as the N-1 Security and Chance-Constrained Unit Commitment (SCCUC) problem.

A preliminary version of this model appears in our conference paper (Sundar et al. (2016)). The conference paper presented three different algorithms to solve the problem on an IEEE RTS-96 one-area system; however the algorithms do not scale for larger systems. *The introduction of discrete variables to the model, among other important modeling details, makes this problem much more difficult to solve than the original single-period formulation discussed in (Bienstock et al. (2014))*. In this paper, we focus on addressing the computational issues associated with scalability with a new, modified Benders decomposition algorithm. From a scaling perspective, other stochastic UC models can handle problems with 225 and 118 buses (Papavasiliou and Oren (2013) and Wang et al. (2012), respectively). While these models are comparable in size to our own, they do not include N-1 security, which increases the size of the problem by an order of magnitude. Thus, we argue that our model and approach is more scalable than these prior approaches.

2. Related Work

We now review the models and algorithms that have addressed variations of unit commitment and optimal power flow problems that are most similar to the SCCUC. In Papavasiliou and Oren (2013), a stochastic UC variant with generator and line contingencies was considered. The authors develop a two-stage,

dual-decomposition algorithm that includes wind with a scenario-based approach. The approach was tested on a 225-bus model of the California power system and the average computation time for solving a 42-scenario model was approximately 6 hours. A variation of this problem was studied in Wang et al. (2012), with generation reserves modeling and in Margellos et al. (2013), without generation reserves modeling. Here, the authors also developed a sampling-based approach to account for wind uncertainty with a chance-constrained formulation. They compared their algorithms, using Monte Carlo simulations, with a deterministic variant on a modified IEEE 118-bus network and the IEEE 30-bus network, respectively. Pandzic et al. (2015) developed a transmission-constrained UC formulation where the wind uncertainty is modeled using an interval formulation. They compared the solution cost and robustness of their approach with existing stochastic, interval and robust UC techniques on the IEEE RTS-96 test system. Finally, Zhao et al. (2013) developed a multi-stage robust UC formulation that considers uncertainties due to both demand and wind and tested the effectiveness of the algorithm on the IEEE 118-bus system.

Within the literature, the number of papers that consider stochastic versions of UC with N-1 contingency modeling is limited. For example, the chance-constrained OPF problem of Vrakopoulou et al. (2013b) incorporates both wind and N-1 security constraints, but omits UC modeling, thus reducing the problem complexity. Nasri et al. (2014) develop a Benders decomposition algorithm to solve the UC with wind uncertainty and AC power-flow constraints, but omits the N-1 contingency modeling. Vrakopoulou et al. (2013b) and Nasri et al. (2014) study the effectiveness of their proposed approaches on the IEEE 30-bus and IEEE 96-RTS one area system, respectively. Moreira et al. (2015) develop a Benders decomposition algorithm for the UC with N-1 contingency modeling, reserve modeling, uncertainty in demands and illustrate their algorithm on a 3-bus and the IEEE 24-bus systems. Pozo and Contreras (2013) develop a chance constrained model with $n-k$ security criterion; they handle the chance constraints by drawing 100 samples from the probability distribution for wind and enforce the hard constraints on all the 100 scenarios. Their algorithms are tested on a 3-bus and a 10-bus model. In terms of model comprehensiveness, the model most similar to ours is that of Bertsimas et al. (2013). They developed a two-stage, adaptive robust UC model with security constraints and nodal net injection uncertainty. The model includes a deterministic uncertainty set, unlike the probability distribution of this paper, to model the wind. They proposed a Benders-based decomposition algorithm to handle line contingencies over a large-scale system, however they do not consider generator contingencies. It is the combination of both types of contingencies, especially the generator contingencies with reserve modeling, that makes our problem closer to the necessities of an Independent System Operator (ISO) and a lot more difficult to solve.

In this paper, we formulate SCCUC as a large Mixed-Integer Second-Order Cone Program (MISOCP) that leverages the recent work in Bienstock et al. (2014), Lubin et al. (2016), Roald et al. (2013). This formulation models two kinds of reserves, generator reserves and tertiary/spinning reserves. These reserves

respond to wind fluctuations and outages, respectively. We develop a sequential, modified Benders decomposition algorithm that exploits the block diagonal structure of the constraint matrix. The decomposition algorithm solves an inner problem that accounts for generator contingencies using a Benders decomposition. The outer loop accounts for line contingency constraints which are modeled as Second-Order Cones (SOCs) and efficiently solved via an outer-approximation technique. Our algorithm is parallelizable and extensive computational experiments based on the three area IEEE RTS-96 system (see Wong et al. (1999)) and IEEE 300 NESTA test system (see Coffrin et al. (2014)) are used to demonstrate the effectiveness of the algorithm. We also present a detailed comparison of the SCCUC formulation to the deterministic variant of the problem to illustrate the economic and operational advantages of the SCCUC.

3. Problem Formulation

Throughout this paper we utilize the linearized DC power flow model. While this model has many limitations, it is the model most generally used in the UC literature. In order to isolate the primary complexities (due to chance-constrained response of wind fluctuations and the combinatorial explosion of solutions) and highlight this paper's core algorithmic contributions, we adhere to the traditional UC model with linearized DC power flow equations. Future work will need to consider more realistic power flow models and develop tractable chance-constrained formulations on models of the nonlinear power flow physics. Reference (Lubin et al. (under review)) is a good starting point for developing these models.

3.1. Nomenclature

Sets:

$\mathcal{B}$ - set of buses, indexed by b

$\mathcal{L}$ - set of lines, indexed by ℓ

$\mathcal{G}$ - set of generators, indexed by i

$\mathcal{S}_i$ - set of start-up cost blocks for generator i, indexed by s

$\mathcal{K}$ - set of generator cost blocks for generator i, indexed by k

$\mathcal{W}$ - set of buses with wind generation

$\mathcal{T}$ - set of discretized times (hours), indexed by t

C_g - set of generator contingencies, indexed by gc

C_ℓ - set of line contingencies, indexed by lc

Binary decision variables:

$x_i(t)$ - generator on-off status at time t

$y_i(t)$ - generator 0-1 start-up status at time t

$z_i(t)$ - generator 0-1 shut-down status at time t

$w_{is}(t)$ - generator 0-1 status if i starts at time t after being down for s hours

Continuous decision variables:

$sc_i(t)$ - start-up cost of i at time t, \$

$p_i(t)$ - power output of i at time t, MW

$r_i^+(t)$, $r_i^-(t)$ - up-reserve and down-reserve power output of i at time t, MW

$r_i^{up}(t)$ - tertiary reserve power output of i at time t, MW

$g_i^k(t)$ - power output on segment k of cost curve of i at time t, MW

$\alpha_i(t)$ - participation factor of controllable generator i at time t

$f_\ell(t)$ - real power flow of ℓ at time t, MW

$\delta_i^{gc}(t)$ - power provided by i for contingency gc at time t, MW

$f_\ell^{gc}(t)$ - power flow on ℓ for contingency gc at time t, MW

$f_\ell^{\ell c}(t)$ - power flow on ℓ for contingency ℓc at time t, MW

Parameters:

β_ℓ - susceptance of line ℓ

$p_i^{\min}$, $p_i^{\max}$ - minimum and maximum output of generator i, MW

$p_{i,k}^{\max}$ - maximum output of generator i in production cost block k, MW

$d_b(t)$ - demand at bus b for hour t, MW

a_i^0 - no-load cost of the generator i, \$

a_i^1 - linear cost coefficient for r_i^+ and r_i^- for generator i, \$/MW

a_i^2 - linear cost coefficient for r_i^{up} for generator i, \$/MW

K_i^k - slope of the k^{th} segment of the cost curve for i, \$/MW

$f_\ell^{\max}$ - capacity of line ℓ, MW

$\overline{L}_i$ - min. time i has to run, hrs

$\underline{L}_i$ - min. time i has to be off, hrs

UT_i, DT_i - minimum up-time and down-time of generator i, hrs

$p_i^{\text{up,init}}$, $p_i^{\text{down,init}}$ - number of time periods generator i has been on and off before $t = 0$, hrs

$p_i^{\text{on-off}}$ - on-off status of generator i at $t = 0$

$p_i(0)$ - power output of generator i at $t = 0$, MW

RU_i, RD_i - ramp-up and ramp-down limit of generator i, MW/hr

c_{is} - cost of block s of stepwise start-up cost function of i, \$

$\overline{T}_{is}$, $\underline{T}_{is}$ - upper and lower limit of block s of the start-up cost of generator i, hrs

$\mu_b(t)$ - output of wind farm at b for time t, MW

$\theta_b(t)$ - phase angle at bus b at time t,

$\omega_b(t)$ - actual wind deviations from forecast $\mu_b(t)$, at time t

r - index of the reference bus

R - bounds on the reserves that can be purchased, MW

B - bus admittance matrix

In the rest of the article, bold symbols denote random variables. In particular, $\boldsymbol{\omega}_b(t)$ is the random variable that models $\omega_b(t)$ for hour t. In the SCCUC, we assume that the deviations, $\boldsymbol{\omega}_b(t)$ are independent and normally distributed with zero mean and variance $\sigma_b(t)^2$ (see Bienstock et al. (2014)). The model can include correlations across space, geographically, in $\boldsymbol{\omega}_b(t)$ similar to the models in (Lubin et al. (2016), Roald et al. (2016)). These wind deviations drive the random fluctuations of the controllable injections $\boldsymbol{p}_i(t)$, and line flows $\boldsymbol{f}_\ell(t)$. We remark that, though we assume the wind power generation to have a normal distribution, conservative choices for the parameters of the distribution can ensure that the chance constraints are satisfied when the wind follows other distributions, as shown Sec. 5.4.

Finally, we let $\Omega(t) = \sum_{b\in\mathcal{W}} \boldsymbol{\omega}(t)$ denote the total deviation in the wind from the forecast. For notational convenience, we use $\bar{p}(t)$, $\bar{\mu}(t)$, $\bar{d}(t)$, $\bar{\omega}(t)$, $\bar{\delta}^{gc}(t)$, $\bar{\alpha}(t)$, $\bar{r}^{+}(t)$, $\bar{r}^{-}(t)$, $\bar{r}^{up}(t)$ to denote the vector of power generation, constant wind forecast, demands at the buses, wind deviations, additional generation during generator contingencies, participation factors of the controllable generators, generation up and down reserves and tertiary reserves, respectively.

3.2. Generation control

Since secure operation of the power system requires balance between produced and consumed power at all times, any deviation must be balanced by an adjustment in the controllable generation. We model these adjustments through an affine policy, reflecting automatic generation control (AGC), which establishes power balance within tens of seconds (see Wood and Wollenberg (2012)):

$$\boldsymbol{p}_i(t) = p_i(t) - \alpha_i(t)\Omega(t). \tag{1}$$

Here, $\alpha_i(t) \geqslant 0$ is the participation factor for the controllable generator i. When $\sum_i \alpha_i(t) = 1$, Eq. (1) guarantees balance of generation and load for every time period t. Interestingly, in many applications and utilities, changing $\bar{\alpha}(t)$ is restricted for each generator $i\mathcal{G}$. We remark that computation can be considerable simplified by assuming $\bar{\alpha}(t)$ is a constant or does not vary over t. However, this is not economically advantageous (see Wood and Wollenberg (2012), Bienstock et al. (2014)) and hence, we let $\alpha_i(t)$ be a variable for every generator $i \in \mathcal{G}$ and time period t.

3.3. Reserve generation

In the SCCUC, we model two types of reserves: generation reserves $(r_i^+(t), r_i^-(t))$ and tertiary reserves $(r_i^{up}(t))$. Generation reserves are used to respond to wind fluctuations according to the affine control policy in (1) and the tertiary reserves are used to respond to generator outages. The linear cost coefficients for purchasing generation reserves and tertiary reserves from a generator i at time t are given by a_i^1 and a_i^2, respectively.

3.4. Line flows

The random fluctuations in line flows, $\boldsymbol{f}_\ell(t)$, for line ℓ depend on the wind fluctuations implicitly through the random bus phase angles $\boldsymbol{\theta}_b(t)$, i.e.

$$\bar{p}(t) + \bar{\mu}(t) - \bar{d}(t) + \bar{\omega}(t) - \Omega(t)\bar{\alpha}(t) = B\boldsymbol{\theta}(t). \tag{2}$$

The bus admittance matrix B is invertible after removing the row and column corresponding to the reference bus $r \in \mathcal{B}$. Following the DC power flow model in Wood and Wollenberg (2012), the flows $\boldsymbol{f}_\ell(t)$ are linear functions of the bus phase angles, hence we denote the $|\mathcal{L}| \times |\mathcal{B}|$ matrix M as the linear map from power injections to line flows. Then, the random line flows for each line ℓ are computed as:

$$\boldsymbol{f}_\ell(t) = M_{(\ell,\cdot)} \left(\bar{p}(t) + \bar{\mu}(t) - \bar{d}(t) + \bar{\omega}(t) - \Omega(t)\bar{\alpha}(t)\right). \tag{3}$$

3.5. Post generator contingencies

Generator i's output after the outage of a generator gc during hour t is modeled as

$$p_i^{gc}(t) = p_i(t) + \delta_i^{gc}(t) \tag{4}$$

To ensure power balance we enforce

$$\sum_{i \in \mathcal{G}} \delta_i^{gc}(t) = 0, \text{ and } \delta_{gc}^{gc}(t) = -p_{gc}(t) \tag{5}$$

We remark that we ignore the impact of wind fluctuations and loss of activated generation reserves during generator outages. This leaves an increased risk of post-contingency line overloading and possibly an increased loading on the generators. However, we assume that the probability of a large generation outage happening simultaneously with a large wind deviation is a rare event and is outside the scope of normal N-1 security assessment. Under this assumption, the post generator contingency line flows are deterministic, i.e.

$$f_\ell^{gc}(t) = M_{(\ell,\cdot)} \left(\bar{p}(t) + \bar{\delta}^{gc}(t) + \bar{\mu}(t) - \bar{d}(t)\right) \tag{6}$$

where M is the matrix defined in Sec. 3.4 and $f_\ell^{gc}(t)$ is the line flow on the line ℓ post generator outage gc at time t.

3.6. Post line contingencies

A line outage changes the topology of the system; it changes the matrix M defined in Sec. 3.4. Let $M^{\ell c}$ denote the matrix M corresponding to the topology after a line outage ℓc. Using these notations, we model the line flow during a line contingency, ℓc, as follows:

$$\boldsymbol{f}_\ell^{\ell c}(t) = M_{(\ell,\cdot)}^{\ell c} \left(\bar{p}(t) + \bar{\mu}(t) - \bar{d}(t) + \bar{\omega}(t) - \Omega(t)\bar{\alpha}(t)\right) \tag{7}$$

where, $\boldsymbol{f}_\ell^{\ell c}(t)$ is the random line flow on ℓ during contingency ℓc at time t. Unlike generator outage contingencies, here the normal operation generation levels are not modified. We also ensure that random line flows before and after the outage do not exceed thermal limits with high probability as discussed in Sec. 3.7.6.

3.7. Optimization problem

With the notations and modeling considerations in Sec. 3.1 – 3.6, we next present the formulation of the SCCUC. The objective function of the SCCUC minimizes the operating cost of the generators. The cost includes no-load cost, start-up cost, the running cost of all the generators and the cost of the generation and tertiary reserves, i.e.

$$\min \sum_{i\in\mathcal{G}} \sum_{t\in\mathcal{T}} \Big\{ a_i^0 \cdot x_i(t) + \sum_{k\in\mathcal{K}} K_i^k \cdot g_i^k(t) + sc_i(t) + \big[a_i^1 \cdot (r_i^+(t) + r_i^-(t)) + a_i^2 \cdot r_i^{up}(t) \big] \Big\} \tag{8}$$

The objective function is motivated by the models in Pandzic et al. (2015), Padhy (2004), Wang et al. (2008). The optimization is subject to constraints (1)-(7) and the following constraints:

3.7.1. Binary variable logic

$$y_i(t) - z_i(t) = x_i(t) - x_i(t-1) \quad \forall t \in \mathcal{T}, i \in \mathcal{G}, \tag{9}$$

$$y_i(t) + z_i(t) \leqslant 1 \quad \forall t \in \mathcal{T}, i \in \mathcal{G}. \tag{10}$$

Constraint (9) determines if the generator is started up or shut down at hour t based of its on-off status between hour t and $t-1$. Constraint (10) ensures that a generator i is not started up and shut down in the same hour t.

3.7.2. Generation limits

$$0 \leqslant r_i^-(t), r_i^+(t), r_i^{up}(t) \leqslant R \cdot x_i(t) \quad \forall i \in \mathcal{G}, t \in \mathcal{T}, \tag{11}$$

$$\delta_i^{gc}(t) \leqslant r_i^{up}(t) \quad \forall i \in \mathcal{G}, t \in \mathcal{T}, gc \in C_g, \tag{12}$$

$$\sum_{n\in\mathcal{G}} r_n^{up}(t) \geqslant p_i(t) \quad \forall i \in \mathcal{G}, t \in \mathcal{T}, \tag{13}$$

$$p_i(t) - r_i^-(t) \geqslant p_i^{\min} \cdot x_i(t) \quad \forall i \in \mathcal{G}, t \in \mathcal{T}, \tag{14}$$

$$p_i(t) + r_i^+(t) + r_i^{up}(t) \leqslant p_i^{\max} \cdot x_i(t) \quad \forall i \in \mathcal{G}, t \in \mathcal{T}, \tag{15}$$

$$\Pr(r_i^-(t) \geqslant \Omega(t)\alpha_i(t)) \geqslant 1 - \varepsilon_i \quad \forall i \in \mathcal{G}, t \in \mathcal{T}, \tag{16}$$

$$\Pr(r_i^+(t) \geqslant -\Omega(t)\alpha_i(t)) \geqslant 1 - \varepsilon_i \quad \forall i \in \mathcal{G}, t \in \mathcal{T}, \tag{17}$$

$$0 \leqslant \alpha_i(t) \leqslant x_i(t) \quad \forall i \in \mathcal{G}, t \in \mathcal{T}. \tag{18}$$

The constraints in (11) – (15) enforce the generation limits and the reserve capacity limits for the generator i at every hour t. In particular, constraint (13) ensures that the total tertiary reserves from all the generators during an hour t must be greater than the maximum power generated by any generator during that hour. This guarantees that enough tertiary reserves are purchased at each hour to cover any generator outage. The constraints in (16) – (17) are the chance constraints on the generation limits. They ensure that generation reserves respond to wind fluctuations feasibly with high probability. We do not model the system (emergency) response when these constraints are violated, rather, we limit the probability of having to invoke an emergency control due to a physical limit being reached via a user-specified parameter ε_i for each generator i. Constraint (18) imposes bounds on the participation factors of generators.

3.7.3. Piecewise linear production cost of the generators

$$p_i(t) = \sum_{k \in \mathcal{K}} g_i^k(t) \quad \forall i \in \mathcal{G}, t \in \mathcal{T}, \tag{19}$$

$$0 \leqslant g_i^k(t) \leqslant p_{i,k}^{\max} \cdot x_i(t) \quad \forall i \in \mathcal{G}, t \in \mathcal{T}, k \in \mathcal{K}. \tag{20}$$

Constraint (19) defines the power generated by each generator i at each hour t as the sum of power generated on each block of the production cost curve. Constraint (20) enforces the limits on the power generated on each block.

3.7.4. Stepwise start-up cost of the generators

$$\sum_{s \in \mathcal{S}_i} w_{is}(t) = y_i(t) \quad \forall i \in \mathcal{G}, t \in \mathcal{T}, \tag{21}$$

$$w_{is}(t) \leqslant \sum_{\underline{T}_{is}}^{\overline{T}_{is}} z_i(t-s) \quad \forall i \in \mathcal{G}, t \in \mathcal{T}, s \in \mathcal{S}_i, \tag{22}$$

$$sc_i(t) = \sum_{s \in \mathcal{S}_i} w_{is}(t) \cdot c_{is} \quad \forall i \in \mathcal{G}, t \in \mathcal{T}. \tag{23}$$

The start-up cost for generator i varies with the number of consecutive time periods it has been switched off before it is started up. Constraint (21) ensures exactly one start-up cost from the set of start-up cost blocks is chosen for generator i. Constraint (22) identifies the appropriate start-up block by implicitly counting the number of consecutive time periods the generator has been in the off state. Finally, constraint (23) selects the actual start-up cost for the objective function.

3.7.5. Minimum up and down-time, ramping consraints

$$x_i(t) = p_i^{\text{on-off}} \quad \forall i \in \mathcal{G}, t \leqslant \overline{L}_i + \underline{L}_i, \tag{24}$$

$$\sum_{n=\overline{t}}^{t} y_i(n) \leqslant x_i(t) \quad \forall i \in \mathcal{G}, t \geqslant \overline{L}_i, \overline{t} = t - UT_i + 1, \tag{25}$$

$$\sum_{n=\underline{t}}^{t} z_i(n) \leqslant 1 - x_i(t) \quad \forall i \in \mathcal{G}, t \geqslant \underline{L}_i, \underline{t} = t - DT_i + 1, \tag{26}$$

$$RD_i \geqslant p_i(t-1) - p_i(t) \quad \forall i \in \mathcal{G}, t \in \mathcal{T}, \tag{27}$$

$$RU_i \geqslant p_i(t) - p_i(t-1) \quad \forall i \in \mathcal{G}, t \in \mathcal{T}. \tag{28}$$

The constraint in Eq. (24) sets the on-off status of generator i based on initial conditions. Notice that both $\underline{L}_i$ and $\overline{L}_i$ will not take positive values simultaneously. The constraints in Eqs. (25) and (26) enforce minimum up-time and minimum down-time constraints for generator i for the remaining time intervals of the planning horizon. The constraints (27) and (28) enforce ramping limits on consecutive periods on every generator i.

3.7.6. Power flow constraints

$$\sum_{i\in\mathcal{G}} \alpha_i(t) = 1, \alpha_r(t) = 0 \quad \forall t \in \mathcal{T}, \tag{29}$$

$$\sum_{b\in\mathcal{B}} (p_b(t) + \mu_b(t) - d_b(t)) = 0 \quad \forall t \in \mathcal{T}, \tag{30}$$

$$\sum_{i\in\mathcal{G}} \delta_i^{gc}(t) = 0 \text{ and } \delta_{gc}^{gc}(t) = -p_{gc}(t) \quad \forall t \in \mathcal{T}, gc \in C_g, \tag{31}$$

$$\Pr(\boldsymbol{f}_\ell(t) \leqslant f^{\max}) > 1 - \varepsilon_\ell \quad \forall \ell \in \mathcal{L}, t \in \mathcal{T}, \tag{32}$$

$$\Pr(\boldsymbol{f}_\ell(t) \geqslant -f^{\max}) > 1 - \varepsilon_\ell \quad \forall \ell \in \mathcal{L}, t \in \mathcal{T}, \tag{33}$$

$$\Pr(\boldsymbol{f}_\ell^{\ell c}(t) \leqslant f^{\max}) > 1 - \varepsilon_\ell^{\ell c} \quad \forall \ell \in \mathcal{L}, t \in \mathcal{T}, \ell c \in C_\ell, \tag{34}$$

$$\Pr(\boldsymbol{f}_\ell^{\ell c}(t) \geqslant -f^{\max}) > 1 - \varepsilon_\ell^{\ell c} \quad \forall \ell \in \mathcal{L}, t \in \mathcal{T}, \ell c \in C_\ell, \tag{35}$$

$$-f^{\max} \leqslant f_\ell^{gc}(t) \leqslant f^{\max} \quad \forall \ell \in \mathcal{L}, t \in \mathcal{T}, gc \in C_g. \tag{36}$$

The power flow equations are adapted from (Bienstock et al. (2014), Lubin et al. (2016), Roald et al. (2016)) and are generalized for multiple time periods. Constraint (29) guarantees balance of generation and load via the participation factors (Sec. 3.2). Constraints (30) and (31) impose the demand-generation balance during normal operations and contingencies for all time periods. Finally, constraints (32) – (35) are the chance constraints for the line flows during normal operations and during line contingencies. ε_ℓ and $\varepsilon_\ell^{\ell c}$ are user-defined parameters to control to probability of line violations during normal operations and post line contingencies, respectively. Constraint (36) imposes hard line limits on the lines for post generator contingencies; $\boldsymbol{f}_\ell$ and $\boldsymbol{f}_\ell^{\ell c}$ are computed using equations (3) and (7) respectively.

3.8. Reformulation of Chance Constraints

The chance constraints in (16), (17), (32) - (35) are often non-convex and difficult to handle. But, under the assumption of normality, these equations can be reformulated to a convex form that is computationally tractable (see Bienstock et al. (2014), Lubin et al. (2016), Roald et al. (2013)). In particular, if $\boldsymbol{\xi}$ is a muti-variate normal random variable with mean μ and covariance Σ and if v is the decision variable vector, then a chance constraint of the form

$$\Pr(\boldsymbol{\xi}^T v \leqslant b) \geqslant 1 - \varepsilon \tag{37}$$

is equivalent to

$$\mu^T v + \phi^{-1}(1-\varepsilon)\sqrt{v^T \Sigma v} \leqslant b. \tag{38}$$

In (38), ϕ^{-1} denotes the inverse cumulative distribution function of the standard normal distribution. The constraint (38) is a convex, SOC constraint. We also remark that the chance constraints in (16) and (17)

contain a special structure that enables reformulation to a linear constraint, as noted in Lubin et al. (2016). Specifically, consider the chance constraint in (16) given by

$$\Pr(r_i^-(t) \geqslant \Omega(t)\alpha_i(t)) \geqslant 1-\varepsilon_i \quad \Rightarrow \quad \Pr(r_i^-(t) - \Omega(t)\alpha_i(t) \geqslant 0) \geqslant 1-\varepsilon_i.$$

In this constraint, $\Omega(t)$ is the total deviation from the forecast which is a Gaussian random variable with mean $\sum_{b\in\mathcal{W}} \mu_b(t)$ and variance $e^T\Sigma(t)e$ (e denotes a vector of ones). Using the above notations, the chance constraint is equivalent to the following linear constraint:

$$r_i^-(t) - \left(\sum_{b\in\mathcal{W}} \mu_b(t)\right)\alpha_i(t) + \phi^{-1}(1-\varepsilon_i)\alpha_i(t)\sqrt{e^T\Sigma(t)e} \leqslant 0. \tag{39}$$

We remark that a similar reduction holds for the chance constraint in (17).

4. Solution Methodology

In this section, we present our modified Benders decomposition algorithm to solve the SCCUC problem. For the purposes of our algorithm, we classify the constraints into three categories:

(A) Normal operation, unit commitment constraints: Constraints (9) – (11), (14), (16) – (30), (32), and (33),

(B) Line contingency constraints: Constraints (34) and (35)

(C) Generator contingency constraints: Constraints (12), (13), (15), (31), and (36).

The resulting SCCUC problem is a large, MISOC problem. Even large-scale continuous SOC problems are often difficult for commercial solvers (despite their nice theoretical properties). Hence, we use a sequential outer-approximation technique to handle the SOC constraints. This approach was effective on similar problems in transmission systems (see Bienstock et al. (2014) and Nagarajan et al. (2016) for SOCP and MISOCP, respectively).

4.1. Modified Benders decomposition

While a Generalized Benders decomposition algorithm based on SOCP duality exists for the SCCUC (see Sundar et al. (2016)), the approach has convergence and numerical issues for even medium sized test instances. The convergence issues are due to the line contingency chance constraints in category (B); the number of line contingency chance constraints is $(|\mathcal{L}|-1)\times|\mathcal{L}|\times|\mathcal{T}|$. Sundar et al. (2016) formulated the constraints in category (B) as Benders feasibility sub-problems and generated feasibility cuts using SOC duality theory. The main challenge with this approach is that current state-of-the-art SOC programming solvers are not mature enough to give reliable extreme rays for infeasible SOC programs. We remark that this is just a practical implementation issue and not a theoretical one. The alternative is to add all the constraints in category (B) to the Benders master problem and perform sequential outer-approximation on these constraints to solve the master problem. This results in a large number of SOC constraints in a Benders master problem, thereby (excessively) increasing the computation time to solve the master problem.

Furthermore, it has been observed that for power-flow based problems in transmission systems and in the presence of wind, the number of SOC constraints in category (B) that actually are tight for the optimal solution obtained by ignoring these constraints are very minimal. Based on these observations, we were motivated to develop a modification to the Benders decomposition algorithm when there are a large number of SOC constraints.

Now, we present a high-level overview of the approach and, in the following sections, we formalize the algorithm. This technique first relaxes the line contingency constraints in category (B) from the SCCUC to obtain a relaxed SCCUC (R-SCCUC) formulation. This R-SCCUC is then decomposed into a MISOC master problem and linear programming sub-problems. The master problem contains all the constraints in category (A) reformulated as SOC constraints. Each sub-problem spans a single time period and consists of all the generator contingency constraints from category (C) for that time period, with the unit commitment variables and generator dispatch variables during normal operating conditions fixed to values obtained from solving the master problem. This relaxed problem (R-SCCUC) is solved using the traditional Benders decomposition algorithm. We now present an overview of the Benders decomposition algorithm in order to keep the presentation self-contained. The optimal solution to the master problem determines the running, start-up and shut-down schedule of the generators with their dispatch during normal operating conditions. For the schedule fixed from the master problem, the Benders sub-problems determine the total generation reserves when a generator outage occurs. The solutions to the sub-problem provide information on the quality of the dispatch decisions made by the master problem. This information is passed to the master problem again as Benders optimality or feasibility cuts. The cuts enable the master problem to modify and compute better dispatch and generation levels. This iterative procedure continues until the Benders decomposition termination condition is satisfied. As for line contingency constraints in category (B), the optimal solution obtained for the R-SCCUC problem via the Benders decomposition is verified to see if it violates any of the these constraints. If so, these infeasible SOC constraints are added to the master problem of the R-SCCUC and the resulting problem is resolved again using the Benders decomposition algorithm. The pseudocode of the modified Benders decomposition algorithm is given in Algorithm 1. We note that the MISOC master problem in the Benders decomposition algorithm is solved via sequential outer-approximation of the SOC constraints.

In summary, the modified Benders decomposition algorithm relaxes a large number of SOC constraints (category (B) constraints) from the SCCUC and solves the resulting R-SCCUC using a combination of sequential outer-approximation and traditional Benders decomposition. The relaxed infeasible SOC constraints is then added back to the R-SCCUC in an iterative fashion with the traditional Benders decomposition in combination with the sequential outer-approximation being used to solve the R-SCCUC during each iteration.

Algorithm 1 Modified Benders Decomposition - Pseudo Code

1: **loop** ▷ Outer loop: Relax category (B) constraints to obtain R-SCCUC
2: Solve master problem (MISOCP) via sequential outer-approximation
3: **loop**
4: Fix master problem variables & solve the sub-problems
5: Generate feasibility and optimality cuts
6: Resolve master problem with the additional cuts
7: Check Benders decomposition termination condition
8: **if** All the category (B) constraints are feasible **then**
9: Exit with optimal solution for SCCUC
10: **else**
11: Augment violated category (B) constraints to R-SCCUC and re-solve (go to step 2).

4.2. Benders sub-problems

The Benders sub-problems are formulated with the unit commitment decisions and the generation level solutions of the master problem and they compute new generation levels for each generator outage. One sub-problem is formulated for each time period and the objective of each sub-problem minimizes the total generation reserves allocated during any generator outage during that time period. For a fixed time period t, the sub-problem is as follows:

$$SP(t,\bar{x}(t),\bar{r}^{+}(t),\bar{p}(t)) : \min \sum_{i\in\mathcal{G}} a_i^2 r_i^{up}(t) \tag{40}$$

subject to

$$0 \leqslant r_i^{up}(t) \leqslant R\cdot x_i(t) \quad \forall i\in\mathcal{G},$$

$$\delta_i^{gc}(t) - r_i^{up}(t) \leqslant 0 \quad \forall i\in\mathcal{G}, gc\in C_g,$$

$$\sum_{n\in\mathcal{G}} r_n^{up}(t) \geqslant p_i(t) \quad \forall i\in\mathcal{G},$$

$$r_i^{up}(t) \leqslant p_i^{\max}\cdot x_i(t) - p_i(t) - r_i^{+}(t) \quad \forall i\in\mathcal{G},$$

$$p_i^{gc}(t) - \delta_i^{gc}(t) = p_i(t) \quad \forall i\in\mathcal{G}, gc\in C_g,$$

$$\sum_{i\in\mathcal{G}} \delta_i^{gc}(t) = 0, \text{ and } \delta_{gc}^{gc}(t) = -p_{gc}(t) \quad \forall gc\in C_g,$$

$$-f^{\max} \leqslant f_\ell^{gc}(t) \leqslant f^{\max} \quad \forall \ell\in\mathcal{L}, gc\in C_g.$$

For ease of exposition and clarity, the sub-problem constraints shown in (40) have the master problem variables on the right-hand side. Each sub-problem is a linear program and the values of the variables $\bar{x}(t)$, $\bar{r}^{+}(t)$ and $\bar{p}(t)$ are obtained from the master problem solution. A Benders feasibility or optimality

cut is generated based on whether the sub-problem is infeasible or optimal, respectively. If we model the constraints of the sub-problem with $A(t)X(t) \leqslant b(t)$, then the Benders optimality cut is given by $\eta(t) \geqslant \gamma(t)^T b(t)$, where $\gamma(t)$ are the dual values of the constraints. Similarly, the the feasibility cut is given by $\beta(t)^T b(t) \leqslant 0$, where $\beta(t)$ is the infeasible ray found using Farkas' lemma. These cuts are added to the master problem and the master problem is resolved (see step 5 and 6 of algorithm 1). The master problem objective value provides a lower bound and an upper bound is computed using the solution to the sub-problems. The inner loop of Algorithm 1 terminates when the gap between the upper and lower bound is within a tolerance value. We remark that during each iteration of the inner loop, $|\mathcal{T}|$ sub-problems are solved to generate the optimality and feasibility cuts.

4.3. Benders master problem

The Benders master problem minimizes the operation costs and generates a schedule of the generators with their power levels during normal operating conditions, i.e.

$$\min \sum_{i\in\mathcal{G}} \sum_{t\in\mathcal{T}} \left\{ a_i^0 \cdot x_i(t) + \sum_{k\in\mathcal{K}} K_i^k \cdot g_i^k(t) + sc_i(t) + \left[a_i^1 \cdot (r_i^+(t) + r_i^-(t)) \right] \right\} + \sum_{t\in\mathcal{T}} \eta(t) \tag{41}$$

subject to

(9) – (11), (14), (16) – (30), (32), and (33),

$$\eta(t) \geqslant \gamma(t)^T b(t) \quad \forall t \in \mathcal{T}, \text{ and} \tag{42}$$

$$\beta(t)^T b(t) \leqslant 0 \quad \forall t \in \mathcal{T}. \tag{43}$$

The variables $\eta(t)$ are surrogate variables introduced in the master problem for each sub-problem and they globally underestimate the value of the generation reserves, $\sum_i r_i^{up}(t)$, for each t. The equations (42) and (43) are the optimality and feasibility cuts generated using the dual value, $\gamma(t)$, and infeasibility ray, $\beta(t)$, for the optimal and infeasible Benders sub-problems.

5. Computational results

In this section, we demonstrate the computational effectiveness of the modified Benders decomposition algorithm to solve the SCCUC and also present the benefits of solving the SCCUC relative to the deterministic version of the unit commitment problem using the three area IEEE RTS-96 system (see Wong et al. (1999)). The comparison between the SCCUC and its deterministic counterpart is based on a variety of factors including nominal operating cost, number of generator and line violations, and amount of generation and tertiary reserves allotted. Generally, there is a lack of established large, test systems for the SCCUC, since, even small problems are hard to solve. Thus, in order to test the scalability of the algorithm for large test cases, we created a modified version of the NESTA IEEE 300 network found in Coffrin et al. (2014). All computational experiments were run on a Intel Haswell 2.6 GHz, 62 GB, 20-core super computing machine at Los Alamos National Laboratory.

5.1. Test system and wind data

The IEEE RTS-96 Wong et al. (1999), modified to accommodate 19 wind farms, was used for empricial testing. The system consists of 73 buses, 120 transmission lines and 96 conventional generators. The total installed capacity of the generators is 10,215 MW. Among the 96 generators, 6 are nuclear and 3 are hydro generators. The NREL Western Wind dataset (Potter et al. (2008)) provides the wind data. Wind farms locations are mapped to the IEEE RTS-96 respecting the lengths of the lines (see Pandzic et al. (2015)). The test system contains a total of 19 wind farms with a total generation capacity of 6900 MW. The locations of the wind farms, the individual generation capacity of each wind farm, the overall system diagram; the step-wise generation cost, start-up cost, ramping restrictions, up and down-time restrictions for each generator; and the load profile data for a 24-hour period used for the case study are in Pandzic et al. (2015) and can be found at `http://www.ee.washington.edu/research/real/library.html`. We use hourly wind forecasts for two sets of 5-day periods for each wind farm provided in Pandzic et al. (2015). Using this forecast data for each 5-day period, the mean and standard deviation of the wind power injection for each time period was estimated assuming that the wind power injections for each hour are independent normally distributed random variables. We classify the wind data sets as favourable and unfavourable; favourable wind data indicates power injections increase with the total load during each time period. Figure 1 shows the total load profile and the sum of the mean wind power injection at the wind farms for both the wind data sets. The cost coefficients a_i^0, a_i^1, and a_i^2 for the generation and tertiary reserves, respectively, are adopted directly from the IEEE RTS-96 generation cost coefficient data and wind power is assumed to have zero marginal cost.

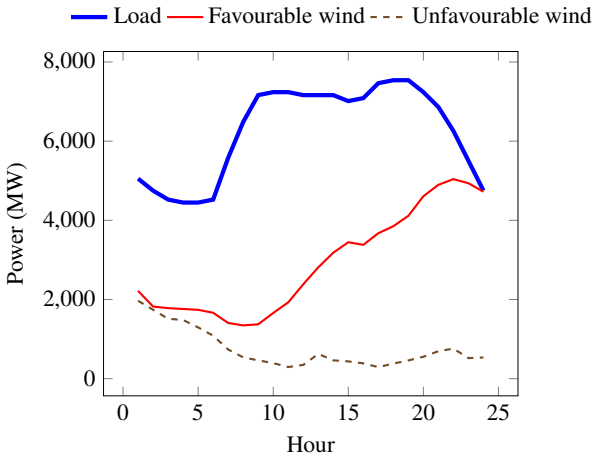

Figure 1 Load profile and mean wind power injection data

5.2. Solving the MISOCP

The MISOCP presented in Sec. 3 for the SCCUC can be directly solved by off-the-shelf commercial solvers like CPLEX or Mosek. Initial numerical simulations indicate that the MISOCP is challenging to solve directly on the three area IEEE RTS-96 test system. For instance, CPLEX 12.7 (IBM (2016)) was not able to produce any feasible solution after running for 2 hours. After presolving the problem in CPLEX, the problem contained 7,123,102 rows, 6,588,222 columns and 184,559,537 nonzeros, 6,273 binaries and 334,920 quadratic constraints. This also motivates the need to develop a specialized algorithm like the modified Benders decomposition algorithm, developed in this paper, to solve the SCCUC (and other two-stage MISOCP problems.

5.3. Performance of modified Benders decomposition algorithm

The SCCUC formulation has three user-defined parameters: $\varepsilon_i,\ \varepsilon_\ell$, and $\varepsilon_\ell^{\ell c}$. For the rest of the computational experiments, we set them to 1%, 10% and 20%, respectively. These are user defined parameters. Based on recent literature, many power system operators do not want generator and transmissions lines violating their production and thermal limits more than 1% and 10% of the time, respectively, during normal operations. In the case of emergency (an $N-1$ failure is an example of an emergency), they permit transmission lines to violate their limits at most 20% of the time (see CIGRE (2009)). We then sequentially vary the loading levels and solve the resulting SCCUC instances using the modified Benders decomposition algorithm in Sec. 4. The nominal load obtained from the data set is assumed to be 100% and the loads are increased by 5% and 10% to stress the system further. For each loading level, both the favourable (F) and unfavourable (UF) wind data sets are used with different penetration rates. For all the runs, the optimality tolerance was set to 1% and the number of threads was set to 4. The algorithms were implemented using the Julia programming language with the JuMP and JuMPChance modeling framework (Dunning et al. (2015)) with CPLEX 12.7 as the commercial solver. The computation times are shown in Figure 2. For all the runs, the modified Benders decomposition algorithm was terminated when the optimality gap was less than 1%. From the figure, it is clear that the algorithm is very effective and is able to provide a feasible solution within 1% of the best lower bound in less than an hour for all the runs. The actual computation times for all the runs is also shown in Tables 1 – 2.

To corroborate the effectiveness of the algorithm from a scalability perspective, we ran the algorithm on an IEEE 300 NESTA test system in Coffrin et al. (2014) that consists of 300 buses, 411 lines, and 57 generators. The wind farm locations, means and variances for each wind farm were generated as follows: all the loads between 80 to 300 MW are assumed to be a wind farm that draws power with a standard deviation equal to 10% of the load at that bus. This results in 51 wind farms. The number of generator and line contingencies in the system is 52 and 411, respectively. 5 generator contingencies are not feasible in this model and were removed. The other unit commitment data that is not available from the IEEE 300

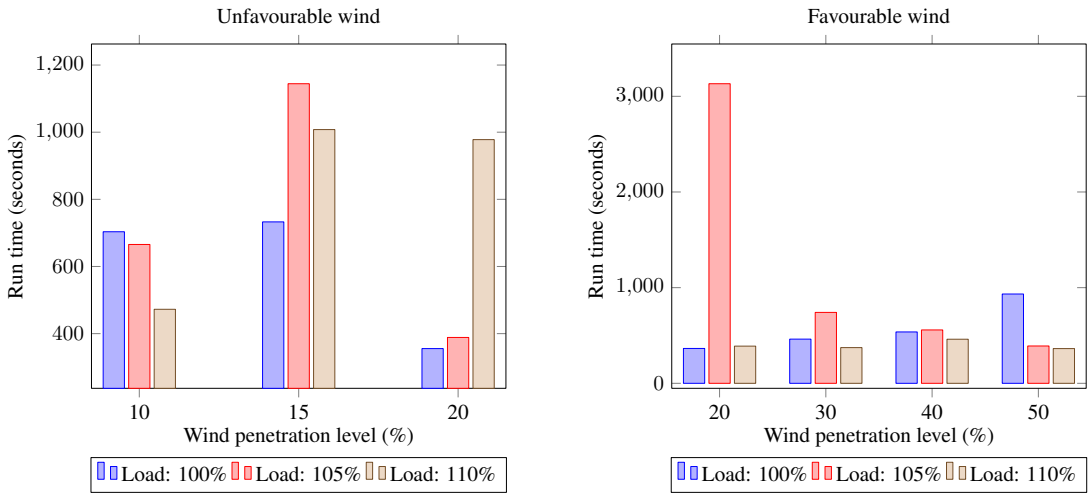

Figure 2 Computation times for the modified Benders algorithm

test system is adapted from IEEE RTS-96 system. The overall run time of the algorithm to converge to a dispatch that is N-1 secure and is within 1% of the optimal dispatch is 3 hours and 25 minutes.

Next, we present the convergence properties of the algorithm. Tables 1 – 2 present the number of iterations of the outer loop of the modified Benders decomposition algorithm (see algorithm 1) and the number of lines that violate the line contingency chance constraints in (34) and (35) after solving the inner problems. This table provides strong evidence of the effectiveness of our approach, as very few lines violate their limits. We remark that the line flow chance constraints for a single line can become infeasible in different time periods; in this case the violation on that line, as presented in the table 1 – 2, is still counted only once. The tables indicate that the modified Benders decomposition is a very effective way of handling chance constraints on the line flow limits during line contingencies, via the outer loop of the algorithm, and converges in a few iterations. It also helps identify the lines that frequently overload in the presence of wind. For instance, the line contingency chance constraints on the lines (107, 108) and (108, 109) in the IEEE RTS-96 were violated after the first iteration of the algorithm 1 during every run.

Table 1 Number of lines on which the contingency line flow chance constraint violations (#CC-V), number of iterations (#I) of the modified Benders decomposition algorithm, and the computation time (seconds) for the modified Benders decomposition algorithm on the instances favourable (F) wind penetration rates.

W%	Load= 100%			Load= 105%			Load= 110%		
F	#CC-V	#I	time	#CC-V	#I	time	#CC-V	#I	time
10	3	2	703.47	3	2	665.57	3	2	472.49
15	5	2	732.82	3	2	1144.37	3	2	1007.79
20	5	2	355.45	3	2	388.62	3	2	977.88

Table 2 Number of lines on which contingency line flow chance constraint violations (#CC-V) and number of iterations (#I) of the modified Benders decomposition algorithm, and the computation time (seconds) for the modified Benders decomposition algorithm on the instances with unfavourable (UF) wind penetration rates.

W%	Load= 100%			Load= 105%			Load= 110%		
UF	#CC-V	#I	time	#CC-V	#I	time	#CC-V	#I	time
20	7	3	364.46	8	4	3131.63	8	2	388.73
30	7	2	461.95	8	2	741.27	7	2	373.30
40	7	2	536.97	7	2	557.93	7	2	460.86
50	4	2	933.50	3	2	390.23	4	2	363.07

5.4. Out-of-sample tests

Next, we study the performance of the dispatch computed by the SCCUC when there are errors in the assumption that the underlying distribution of wind power by performing an out-of-sample test. The formulation and algorithm for the SCCUC assume that the wind power generated is normally distributed (see Dvorkin et al. (2016)), but studies in the literature suggests wind energy distribution does not always follow a normal distribution(Seguro and Lambert (2000)). Here, we test the generation dispatch computed by the SCCUC using forecast of mean wind energy production and variance in wind energy produced by each wind farm (assumption that the wind is normally distributed) against samples from other distributions for the wind power generation. We use samples from the following probability distributions, all with fatter tails than the normal distribution: (i) Laplace, (ii) Logistic, and (iii) Weibull with 2 different shape parameters as in Karki et al. (2006). For the Laplace and Logistic distributions, we match the mean and standard deviation estimated from the forecast data by assuming a normal distribution. For the Weibull distribution, we consider shape parameters $k = 1.2, 2$ and choose the scale parameter to match the standard deviations; the samples are then translated to match the means. The dispatch from the SCCUC is tested against 1000 realizations for each distribution and the maximum empirical violation probabilities, evaluated for each constraint separately, are tabulated in Table 5.4.

We observe that the dispatch obtained using the SCCUC solution performs the worst for the realizations from the Weibull distributions. This is not surprising considering the fact that the Weibull distribution is a bad approximation of a normal distribution. For all the other cases, the maximum probability of violations are well within 1.8% and 20% for the generators and lines, respectively. We note that these violations do not include the ones that occur during single line outages and that similar trends were observed for the line limits during line outages.

We remark that tighter or looser violation probability values ε_i, ε_ℓ with the normal distribution assumption, can be chosen if prior knowledge of the probability distribution of wind is obtained. For instance, if one is certain that the probability distribution of wind is given by a Weibull distribution, the SCCUC can still be utilized by choosing very conservative values for ε_i and ε_ℓ.

Table 3 Maximum violation probability for out-of-sample tests with $\varepsilon_i = 1\%$ and $\varepsilon_\ell = 10\%$ for the dispatch given by the SCCUC.

Distribution	Generators	Lines
Laplace	0.0052	0.0910
Logistic	0.0015	0.0732
Weibull, $k = 1.2$	0.0212	0.2531
Weibull, $k = 2$	0.0181	0.1999

5.5. Comparison of the SCCUC to its deterministic counterpart

From an application standpoint, the comparison between SCCUC and its deterministic counterpart is very valuable for power system operators. The deterministic counterpart assumes $\omega_b(t) = 0$. Both the deterministic and chance constrained unit commitment with N-1 security constraints are solved for a case where the forecast wind power production accounts for 20% of the total load. Since the deterministic unit commitment with N-1 security constraints assumes there are no wind fluctuations, it will not require any generation reserves to handle the wind power fluctuations. In order to make a fair comparison, we assume that the system operator maintains a minimum generation reserve requirement (nominal reserve rule) equal to 0.5% of the load and add this constraint to the optimization problem:

$$\sum_{i\in\mathcal{G}} r_i^+(t) \geqslant 0.005 \cdot \sum_{b\in\mathcal{B}} d_b(t) \quad \forall t \in \mathcal{T} \quad \text{and} \quad \sum_{i\in\mathcal{G}} r_i^-(t) \geqslant 0.005 \cdot \sum_{b\in\mathcal{B}} d_b(t) \quad \forall t \in \mathcal{T}.$$

Furthermore, to obtain a more interesting case, the transmission capacities of the IEEE RTS-96 system were decreased to 90% of their original base case value in Pandzic et al. (2015).

5.5.1. Cost comparison The resulting deterministic unit commitment problem with $N-1$ contingencies is a mixed-integer linear program that is solved using CPLEX 12.7. The time taken by CPLEX to produce a feasible solution with a 1% optimality tolerance for the deterministic problem is 253.53 seconds. The modified Benders decomposition algorithm to solve the SCCUC problem for the same instance is 525.31 seconds. The total cost of the unit commitment and the different cost components are shown in Table 4. We observe that the total cost of the SCCUC solution is almost equal to the cost of its deterministic counterpart. Major differences show up in the cost of generation reserves. The chance constrained model allocates twice as much reserves to handle wind power fluctuations. As mentioned previously the deterministic counterpart is unaware of wind fluctuations and it allocates the bare minimum amount of generation reserves as required by the system operator (0.5% of the load). The difference in the start-up cost for the chance constrained solution is also a result of the higher amount of generation reserves. Larger reserves leads to more generator commitments and higher overall start ups costs. The key observation from Table 4 is that, when the wind penetration is around 20% to 30%, the power generated by wind can be utilized without incurring too much cost-overhead, while keeping the system secure under $N-1$ contingencies.

Table 4 Deterministic vs. Chance-constrained (SCCUC) comparison

	Deterministic	Chance-constrained
Total operational cost ($)	2.025×10^6	2.029×10^6
No load cost ($)	3.141×10^5	3.015×10^5
Start-up cost ($)	14918.5	27077.4
Production cost ($)	1.676×10^6	1.679×10^6
Tertiary reserves cost ($)	19115.2	19141.89
Generation reserves cost ($)	1517.69	2966.60
Optimality gap (%)	0.57	0.38
Generation reserves (MW)	758.84	1483.33

5.5.2. Line and generation limit violations For a system operator, it is also important to reduce the frequency that *any* line or generator limit is violated during a 24-hour period. Fig. 3 compares the number of wind samples realizations out of 1000 that lead to at least one constraint violation during each hour of the day. From Fig. 3, the dispatch obtained from the deterministic problem indicates the empirical probability that at least one constraint is violated during each hour is between 3% and 50%. The solution obtained from the SCCUC has a significantly smaller empirical probability.

Figure 3 The number of wind realizations from the logistic distribution (out of 1000) that lead to one or more constraint violations for the deterministic and the chance-constrained (SCCUC) solutions, respectively.

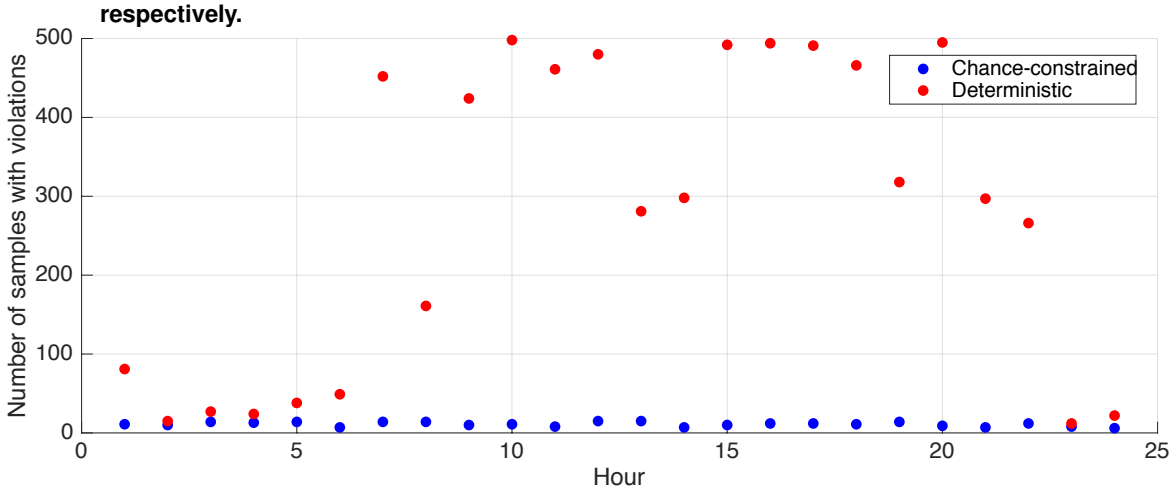

5.6. Influence of wind penetration

To assess the influence of wind power penetration we compare the cost of unit commitment and amount of reserves for varying levels of wind energy penetration. Table 5 shows the variation of the number of committed units, the amount of generation reserves and the total SCCUC cost for different levels of wind penetration. We observe that the increase in the wind penetration levels decrease the overall SCCUC cost. The amount of generation reserves is more or less constant because the variance in the wind deviations is a constant over all instances for this particular study. The decrease in the number of units committed can also

be explained by the fact that power production from the conventional generators in the system decreases with increasing levels of wind penetration.

Table 5 Number of committed units, generation reserves (MW), and SCCUC cost ($) for varying levels of wind penetration

Wind penetration [%]	Committed Units	Generation Reserves [MW]	Total SCCUC Cost [$\times 10^6$\$]	Computation time in seconds
50	699	296.60	1.5656	933.50
40	717	296.63	1.6914	536.97
30	826	296.66	2.0015	461.95
20	923	296.60	2.3509	364.46

6. Conclusion

In this paper, we have presented a MISOCP formulation for the SCCUC problem in the presence of wind fluctuations. To the best of our knowledge, this is the first UC formulation in the literature that includes N-1 security constraints on lines and generators, wind fluctuations, and generator and tertiary reserves. A modified Benders decomposition algorithm is developed to solve the problem. The effectiveness of the approach and its advantages over its deterministic counterpart was demonstrated through extensive computational experiments on a variation of the IEEE RTS-96 system. The results indicate that the proposed formulation is effective and can result in better technical performance including fewer violations of transmission line limits and generator limits during normal operations and during single line or generator outages when compared to its deterministic counterpart. Future work includes generalizations to account for errors in estimating the parameters of the probability distributions for the wind fluctuations and extension of the SCCUC formulation to consider more realistic (AC) power flow models. The work on this problem has also provided motivation to improve the quality of conic optimization solvers and their ability to produce reliable duals. It will also be interesting to understand how the approaches we developed here for the SCCUC could be extended and generalized to other two-stage MISOCP problems.

Acknowledgements

This work was supported by the Advanced Grid Modeling Program of the Office of Electricity within the U.S Department of Energy and the Center for Nonlinear Studies at Los Alamos National Laboratory. We also thank Miles Lubin for his input and contributions on early iterations of these research efforts.

References

(2011) CWE Enhanced Flow-Based MC Feasibility Report. Technical report, Amprion, APX, BelPEX, Creos, Elia, EnBW, EPEX, RTE, Tennet, URL `https://www.epexspot.com/document/12597/CWE_FB-MC_feasibility_report.pdf`.

(2013) Supporting Document for the Network Code on Load-Frequency Control and Reserves. Technical report, ENTSO-E, URL https://www.entsoe.eu/fileadmin/user_upload/_library/resources/LCFR/130628-NC_LFCR-Issue1.pdf.

Andersson G, Donalek P, Farmer R, Hatziargyriou N, Kamwa I, Kundur P, Martins N, Paserba J, Pourbeik P, Sanchez-Gasca J, et al. (2005) Causes of the 2003 major grid blackouts in north america and europe, and recommended means to improve system dynamic performance. *IEEE Trans. Power Systems* 20(4):1922–1928.

Bertsimas D, Litvinov E, Sun XA, Zhao J, Zheng T (2013) Adaptive robust optimization for the security constrained unit commitment problem. *Power Systems, IEEE Trans.* 28(1):52–63.

Bienstock D, Chertkov M, Harnett S (2014) Chance-constrained optimal power flow: risk-aware network control under uncertainty. *SIAM Review* 56(3):461–495.

Bouffard F, Galiana F (2008) Stochastic security for operations planning with significant wind power generation. *IEEE Trans. Power Systems* 23(2):306–316, ISSN 0885-8950, URL http://dx.doi.org/10.1109/TPWRS.2008.919318.

CIGRE (2009) Technical brochure on grid integration of wind generation .

Coffrin C, Gordon D, Scott P (2014) Nesta, the NICTAroad energy system test case archive. *arXiv preprint arXiv:1411.0359* .

Dunning I, Huchette J, Lubin M (2015) JuMP: A modeling language for mathematical optimization. *arXiv:1508.01982 [math.OC]* URL http://arxiv.org/abs/1508.01982.

Dvorkin Y, Lubin M, Backhaus S, Chertkov M (2016) Uncertainty sets for wind power generation. *IEEE Transactions on Power Systems* 31(4):3326–3327.

IBM (2016) IBM ILOG CPLEX Optimizer v12.7. URL http://www-01.ibm.com/software/commerce/optimization/cplex-optimizer.

Karki R, Hu P, Billinton R (2006) A simplified wind power generation model for reliability evaluation. *IEEE Trans. Energy conversion* 21(2):533–540.

Kundur P, Paserba J, Ajjarapu V, Andersson G, Bose A, Canizares C, Hatziargyriou N, Hill D, Stankovic A, Taylor C, Cutsem TV, Vittal V (2004) Definition and classification of power system stability ieee/cigre joint task force on stability terms and definitions. *IEEE Trans. Power Systems* 19(3):1387–1401, ISSN 0885-8950.

Lorca Ã, Sun XA (2015) Adaptive robust optimization with dynamic uncertainty sets for multi-period economic dispatch under significant wind. *IEEE Trans. Power Systems* 30(4):1702–1713.

Lubin M, Bienstock D, Vielma JP (under review) Two-sided linear chance constraints and extensions URL https://arxiv.org/abs/1507.01995.

Lubin M, Dvorkin Y, Backhaus S (2016) A robust approach to chance constrained optimal power flow with renewable generation. *IEEE Transactions on Power Systems* 31(5):3840–3849.

Margellos K, Rostampour V, Vrakopoulou M, Prandini M, Andersson G, Lygeros J (2013) Stochastic unit commitment and reserve scheduling: A tractable formulation with probabilistic certificates. *European Control Conference*, 2513–2518 (IEEE).

Morales J, Conejo A, Perez-Ruiz J (2009) Economic valuation of reserves in power systems with high penetration of wind power. *IEEE Trans. Power Systems* 24(2):900–910, ISSN 0885-8950, URL `http://dx.doi.org/10.1109/TPWRS.2009.2016598`.

Moreira A, Street A, Arroyo JM (2015) Energy and reserve scheduling under correlated nodal demand uncertainty: An adjustable robust optimization approach. *International Journal of Electrical Power & Energy Systems* 72:91–98.

Nagarajan H, Yamangil E, Bent R, Van Hentenryck P, Backhaus S (2016) Optimal resilient transmission grid design. *Power Systems Computation Conference (PSCC), 2016*, 1–7 (IEEE).

Nasri A, Kazempour SJ, Conejo AJ, Ghandhari M (2014) Network-constrained ac unit commitment under uncertainty: A benders' decomposition approach .

Padhy NP (2004) Unit commitment-a bibliographical survey. *Power Systems, IEEE Trans.* 19(2):1196–1205.

Pandzic H, Dvorkin Y, Qiu T, Wang Y, Kirschen DS (2015) Toward cost-efficient and reliable unit commitment under uncertainty .

Papavasiliou A, Oren SS (2013) Multiarea stochastic unit commitment for high wind penetration in a transmission constrained network. *Operations Research* 61(3):578–592.

Potter C, Lew D, McCaa J, Cheng S, Eichelberger S, Grimit E (2008) Creating the dataset for the western wind and solar integration study (usa). *Wind Engineering* 32(4):325–338.

Pozo D, Contreras J (2013) A chance-constrained unit commitment with an $n - k$ security criterion and significant wind generation. *IEEE Transactions on Power systems* 28(3):2842–2851.

Roald L, Misra S, Krause T, Andersson G (2016) Corrective control to handle forecast uncertainty: A chance constrained optimal power flow. *IEEE Transactions on Power Systems* .

Roald L, Oldewurtel F, Krause T, Andersson G (2013) Analytical reformulation of security constrained optimal power flow with probabilistic constraints. *PowerTech (POWERTECH), 2013 IEEE Grenoble*, 1–6 (IEEE).

Seguro J, Lambert T (2000) Modern estimation of the parameters of the weibull wind speed distribution for wind energy analysis. *Journal of Wind Engineering and Industrial Aerodynamics* 85(1):75–84.

Stott B, Alsac O, Monticelli AJ (1987) Security analysis and optimization. *Proceedings of the IEEE* 75(12):1623–1644.

Sundar K, Nagarajan H, Lubin M, Roald L, Misra S, Bent R, Bienstock D (2016) Unit commitment with n-1 security and wind uncertainty. *Power Systems Computation Conference* .

Uçkun C, Botterud A, Birge JR (2016) An improved stochastic unit commitment formulation to accommodate wind uncertainty. *IEEE Trans. Power Systems* 31(4):2507–2517.

Vrakopoulou M, Margellos K, Lygeros J, Andersson G (2013a) A probabilistic framework for reserve scheduling and security assessment of systems with high wind power penetration. *IEEE Trans. Power Systems* 28(4):3885–3896.

Vrakopoulou M, Margellos K, Lygeros J, Andersson G (2013b) Probabilistic guarantees for the n-1 security of systems with wind power generation. *Reliability and Risk Evaluation of Wind Integrated Power Systems*, 59–73 (Springer).

Wang J, Shahidehpour M, Li Z (2008) Security-constrained unit commitment with volatile wind power generation. *Power Systems, IEEE Trans.* 23(3):1319–1327.

Wang Q, Guan Y, Wang J (2012) A chance-constrained two-stage stochastic program for unit commitment with uncertain wind power output. *Power Systems, IEEE Trans.* 27(1):206–215.

Warrington J, Goulart PJ, Mariethoz S, Morari M (2013) Policy-based reserves for power systems. *IEEE Trans. Power Systems* 28(4):4427–4437.

Wong P, Albrecht P, Allan R, Billinton R, Chen Q, Fong C, Haddad S, Li W, Mukerji R, Patton D, et al. (1999) The IEEE reliability test system-1996. A report prepared by the reliability test system task force of the application of probability methods subcommittee. *Power Systems, IEEE Trans.* 14(3):1010–1020.

Wood AJ, Wollenberg BF (2012) *Power generation, operation, and control* (John Wiley & Sons).

Zhao C, Wang J, Watson JP, Guan Y (2013) Multi-stage robust unit commitment considering wind and demand response uncertainties. *Power Systems, IEEE Trans.* 28(3):2708–2717.